

Behavior of Electrodeposited Fe/FeSi Composite in a Static Parallel Magnetic Field

Qiong Long^{1,2,3,*}, Yunbo Zhong³, Yujiao Wu^{2,3}, Yingfen Li^{2,3}, Juan Li^{2,3}

¹ Guizhou Key Laboratory for preparation of light metal materials, Guizhou Institute of Technology Guiyang 550003, China

² Guizhou collaborative innovation center of special function materials, Guiyang 550003, China

³ Shanghai Key Laboratory of Modern Metallurgy and Material Processing, Shanghai University, Shanghai, 200072, China

*E-mail: qiong12030@163.com

Received: 7 June 2019 / Accepted: 6 August 2019 / Published: 30 August 2019

Fe-Si composite coatings were electrodeposited with Fe-30wt%Si or Si particles on low silicon steel strips under a static magnetic field, the direction of imposed magnetic field kept parallel to electric field. The effects of magnetic field on the co-deposition process of magnetic Fe-30wt%Si particles and weak diamagnetic Si particles were investigated. With increasing the magnetic field flux (MFD), the hummocky structures were gradually transformed from the rod-like structures induced in a weak magnetic field. However, bean-like structures on the coating surface of Si particles became more obvious with the increase of MFD. The experimental results revealed that the magnetic property and conductivity of added particles had a great effect on the migration behavior and co-deposition of particles in magnetic fields.

Keywords: Magnetic field; Co-deposition; Fe-Si particle; MHD effect; Filed gradient force

1. INTRODUCTION

Electroplating composite coatings are widely used in industrial applications due to their excellent mechanical and chemical properties, such as hard wearing, corrosion resistance, electrochemical catalysis and photocatalysis[1-4]. Second-phase particles in composite coatings can usually enhance preeminent performance or provide some added specific characters. Therefore, the influence mechanism of particle content and its distribution in coatings has attracted wide attention throughout the world in recent years, and many new modified treatment processes were applied for coating design.

In recent years, magnetic composite electrodeposition has been concerned by more and more researchers worldwide[5-8]. It is generally accepted that the magnetohydrodynamic(MHD) effect

induced by Lorenz force F_L can improve the mass transport markedly [9-10], and the F_L can be expressed as:

$$F_L = J_0 \times B \quad (1)$$

Where J_0 and B are the current density and MFD respectively. The F_L reaches a maximum theoretically when the direction of magnetic field and current array perpendicular each other. Long[11] found that the distribution of Si particles on coating surface was along the direction of MHD flow. During the electroplating process, when the particle and electrode show soft magnetic properties, the particles in electroplating process will migrate to the zone of high gradient magnetic field (∇B) under the gradient field force ($F_{\nabla B}$), and the $F_{\nabla B}$ can be induced:

$$F_{\nabla B} = \chi VB \cdot \nabla B / \mu_0 \quad (2)$$

Where $\mu_0 = 4\pi \times 10^{-7} \text{ V}\cdot\text{s}/(\text{A}\cdot\text{m})$ is the vacuum permeability, the B , χ and V denotes MFD, the magnetic susceptibility and volume of the added particle respectively. Therefore, the $F_{\nabla B}$ increases linearly with the increase of χ or ∇B . Peipmann[12] studied the co-deposition of Al_2O_3 particles coated with a layer of nickel by electroless nickel plating, because of the soft magnetic properties, the $\text{Ni}(\text{Al}_2\text{O}_3)$ particles were tend to migrate to electrode surface under the effect of $F_{\nabla B}$. Thus, when electrodeposition under a magnetic field, the properties of the added particles will have a significant effect on the co-deposition process of the particles. At present, although there are many literatures on electrodeposition under magnetic field, the particles applied in the composite electrodeposition were mainly nano and ceramic particles, and there was very few research literature for the study of composite electrodeposition for conductive or magnetic particles, especially with micron scale. At the same time, the mechanism of the co-deposition process of magnetic particles is not very clear until now.

In this paper, the Fe-Si composite coatings were produced by composite electrodeposition of iron containing silicon-rich particles, and the applied particles were ferromagnetic Fe-30wt%Si particles and weak diamagnetic Si particles with micron scale. The effects of the MFD, the agitate strength and the current density on the behavior of co-deposition process were investigated.

2. EXPERIMENTAL

As experimental raw material, the Fe-30wt%Si alloy particles were produced by vacuum smelting and high-energy ball milling according to Ref.[13]. The average particle size for both the two types of particles was about 2.5 μm , and their diameter distribution was similar and the difference between them can be ignored. Table 1 shows the composition of bath solution, all of the experiment reagents were all analytically pure. The Cl^- not only prevented pure iron anode from passivation, but also improved polarization and modified the layers. Meanwhile, as the dispersing agent, the Hexadecyl trimethyl-ammonium bromide(HTAB) was added to prevent the agglomeration of Fe-Si particles.

In the experiment, the 3.0wt% electrical steel strip was used as cathode(20×30×0.5 mm) and while a pure iron strip (20×30×0.25 mm, Fe 99.99%) was used as anode, and arranged in vertical direction and the distance between electrodes was 20 mm. The pH value was adjusted to 1.5 by H_2SO_4 before depositing, and the particle concentration was kept 20g/L. Meanwhile, to ensure the homogenous suspension of particles in solution, a certain intensity of mechanical agitation was introduced during the

deposition, and deposition temperature was kept at at 25 °C. Furthermore, a magnetic field was imposed in the direction that was parallel to electrolytic current (Figure1).

Table 1 The composition of the bath solution

Component	Concentration (g·L ⁻¹)
NH ₄ ·Cl	23
FeSO ₄ ·7H ₂ O	250
FeCl ₂ ·4H ₂ O	30
HTAB	0.2

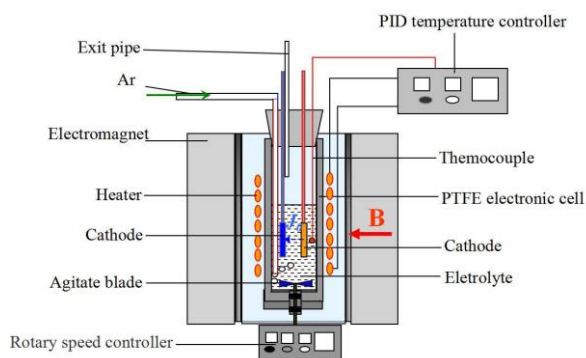


Figure 1. The schematic diagram of the electrodeposition

3. EXPERIMENT RESULTS

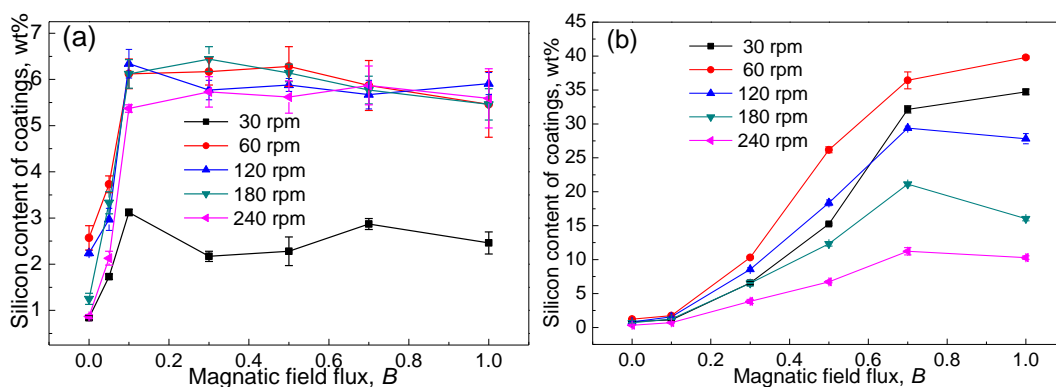


Figure 2. Silicon content of composite coatings at 2 A·dm⁻² in magnetic fields

The silicon content of the composite coatings can be used to characterize the particle content due to the particles added were silicon-rich particles. Figure 2 shows the effects of agitate strength on the silicon content of coatings obtained in magnetic field. With the increase of MFD, the silicon content of coatings reached maximum for Fe-30wt%Si particles when MFD was at 0.1T under the agitate strength of 30-240 rpm. After the agitate strength and the MFD was above 60 rpm and 0.1T, the silicon content

of coatings basically kept constant and which obviously higher than that obtained under a agitate strength of 30 rpm. However, the corresponding silicon content of coatings for the Si particles all showing a maximum when the agitate strength was about 60 rpm under different MFD, and then decreased with continue increasing the agitate strength. Therefore, it can be inferred that the added particles could not totally suspend in solution when the agitate speed was below 60 rpm. After the agitate speed was above the 60 rpm, the agitate strength significantly increased, a scouring action may be induced on the cathode surface and prevented particles from being captured by the subsequent growing metal of reduced iron atom. Therefore, the ideal agitate strength for the following experiments was kept 60 rpm.

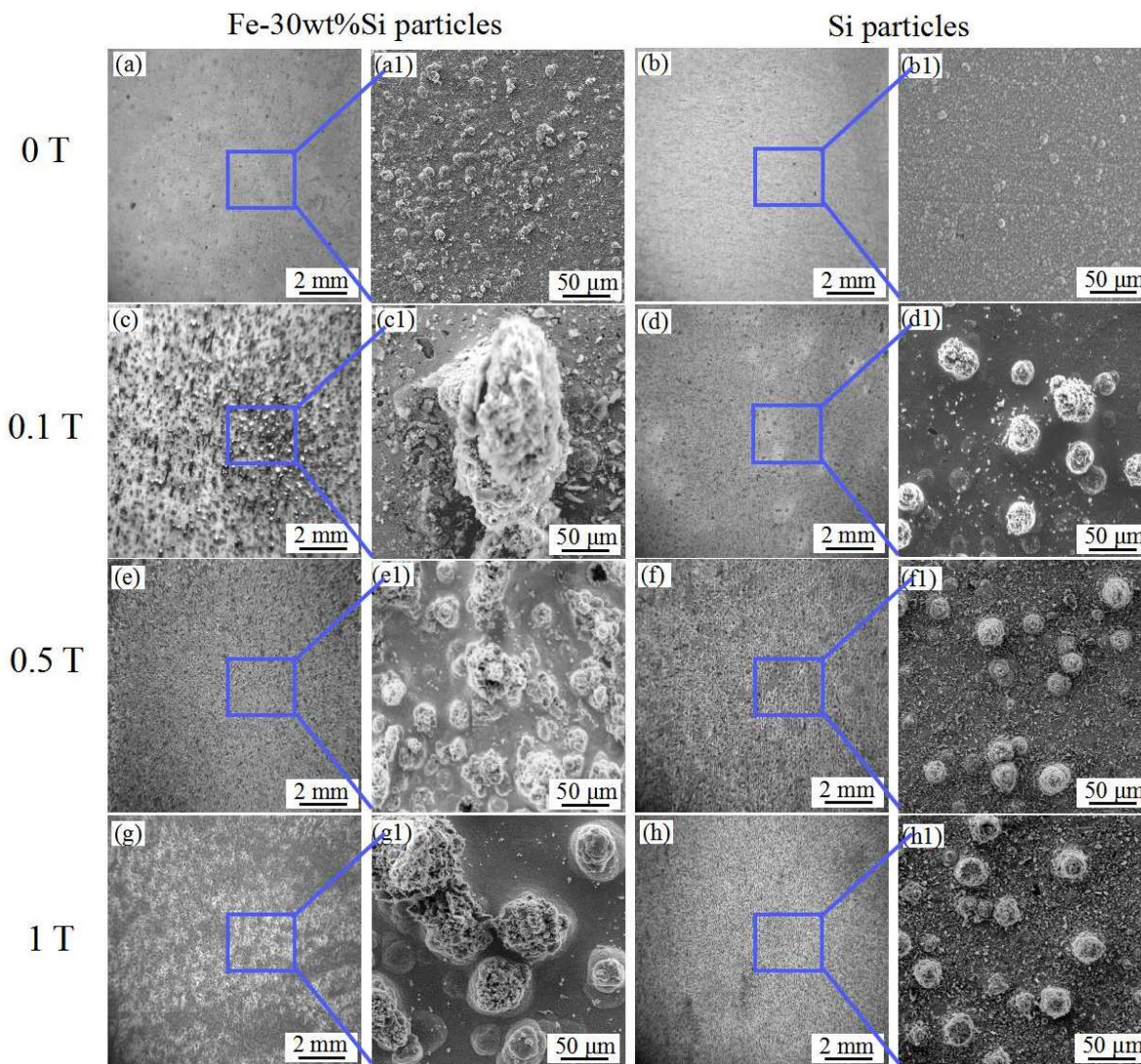


Figure 3. Microstructure of composite coatings for Fe-30wt%Si and Si particles in magnetic fields

The corresponding surface microstructure of composite coatings obtained for was shown in Figure 3. Compared to the relatively flat surface microstructures obtained without external magnetic field(0T), the morphology of coating surface for Fe-30wt% particles became coarse after imposing a weak magnetic field, many rod-like structures were induced and which arrayed in the direction

perpendicular to the coating surface. With the increase of MFD, the rod-like structures weakened, and only small dot microscopic structures existed with magnetic field of 0.5T. When continuing to increase the MFD, the rod-like structures gradually disappeared at macroscopic scale and were totally transformed into the microscopic hummocky structures with diameter of approximately 50 μm under an 1T magnetic field. Simultaneously, bean-like structures appeared on composite coatings of Si particles was becoming increasingly evident with the increase of MFD. Through investigating the surface distribution of elements, it can be confirmed that the hummocky structures contained a large volume of Si element, whereas that for the bean-like structures was main Fe element(Figure 4).

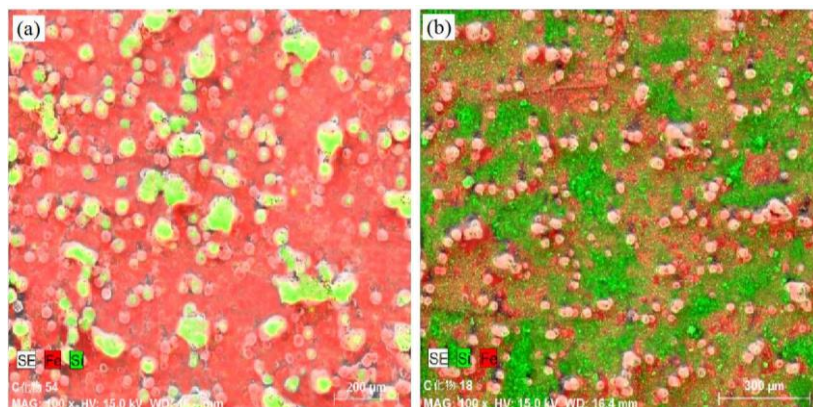


Figure 4. Surface distribution of Fe and Si elements under a 1T magnetic field, the green part stands for the Si and the red stands for Fe

Figure 5 shows the cross-section micrographs of the coatings obtained without and with an 1 T magnetic field. It exhibits that the Fe-30wt%Si particles were inclined to migrate in the central area of the protrusion structures after imposing a 1T magnetic field(Figure 5b), and the incorporated particles on cross-section increased significantly, which was consistent with the surface morphology of the composite coatings. For the Si particles, some protrusions with the small number of Si particles appeared on the cross-section(Figure 5d).

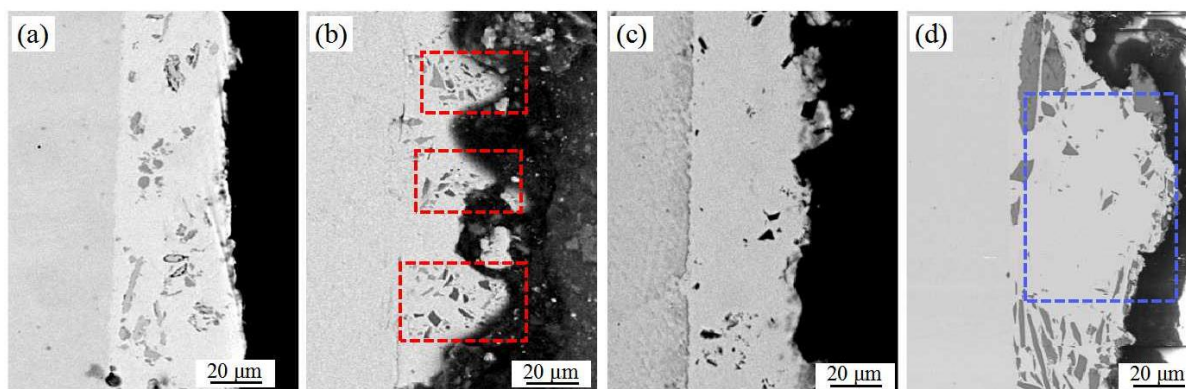


Figure 5. Morphologies of cross-sections of coatings for Fe-30wt%Si and Si particles without and with a 1T magnetic field

4. DISCUSSION

During the composite deposition in magnetic field, the magnetic properties of particles will greatly affect their co-deposition into the coatings. The hysteresis loops of the imposed particles are shown in Figure 6. It can be found that the Fe-30wt%Si particles displayed relatively strong ferromagnetic properties while the Si particles showed weak diamagnetic property. At the same time, the conductive property of the Fe-30wt%Si particles was significantly better than that of Si particles which even showing non-conductive[13-14]. When applying ceramic Si particles, the MHD effect induced by magnetic field and current which can promote the convection and therefore improved the particle content of coatings[11,15-16]. However, when applying the magnetic Fe-30wt%Si particles, according to Equation (2), the $F_{\nabla B}$ acting on magnetic particles should not be ignored.

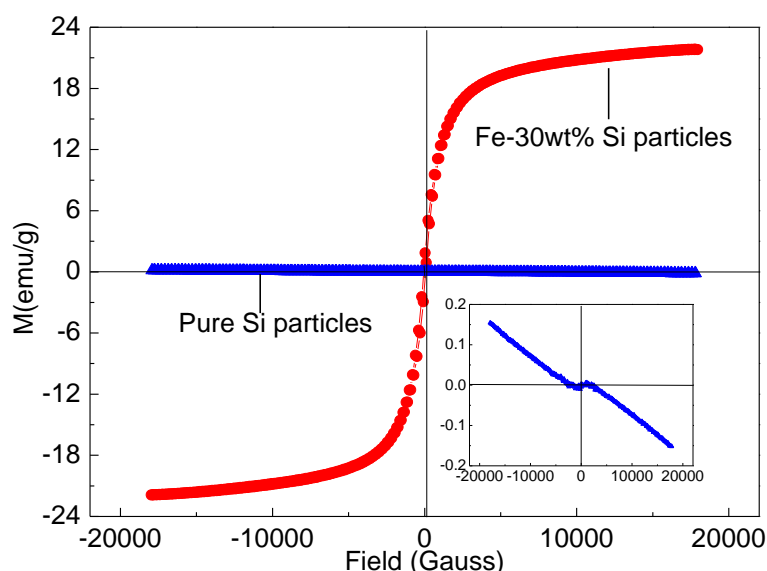


Figure 6. Hysteresis loops of imposed particles

Normally, the distribution of magnetic field flux in the region of stable magnetic field in electromagnet is nearly homogeneous, which means that only exist a very small gradient of magnetic field at most. However, due to the electrode's magnetic properties, an inhomogeneous magnetic field should be induced on the electrode surface after the ferromagnetic electrodes were placed in a static magnetic field. The magnetic flux was distorted and tend to concentrate into the area near electrode surface, and created a strong magnetic gradient ∇B (Figure 7a). When imposing a weak magnetic field, the ferromagnetic Fe-30wt%Si particles in solution will move preferentially towards the locations of higher ∇B . As the result, the 30wt%Si particles will be self-assembled into rod-like structures with a predominant orientation lengthwise along the field direction(Figure 7b).

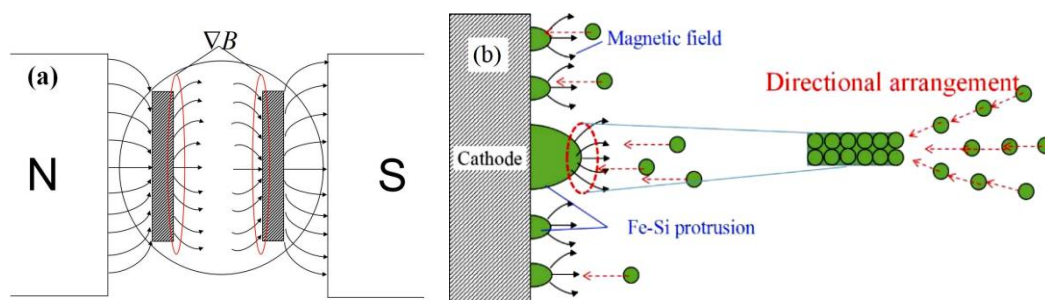


Figure 7. region of ∇B near the electrode(a) and directional arrangement of magnetic field particles(b)

For the cathode, the migration of the particles can enhance the incorporation process of Fe-30wt%Si particles. Simultaneously, a considerable loss of particles will be caused with the migration of Fe-30wt%Si particles towards the anode surface. In addition, the self-assembly of particles also led to a reduction of uniformly suspended particles in solution. As a result, a slight decrease of the co-deposition behavior for Fe-30wt%Si particles on of coatings surface after the MFD was above 0.1 T. With increasing the MFD, the rod-like structures for Fe-30wt%Si particles weakened and totally disappeared when the MFD reached 1T. Obviously, the ∇B in 1T should larger than that of 0.1T, from equation (2), it can be deduced that the rod-like protrusions should not disappear in 1T magnetic field. Therefore, there should exist other dominating factors affecting the co-deposition of Fe-30wt%Si particles. For the Si particles, the phenomenon of rod-like protrusions can be neglected because of the weak diamagnetic properties.

When imposing a parallel magnetic field, the magnetic field kept parallel to electric field at this moment, the Lorentz force should not be generated in theory. However, the current will be distorted from the microcosmic angle in the nearby area of rod-like structures(Figure 8(a)), and formed a current component J_r which was perpendicular to the direction of magnetic field[17-18]. As a result, a Lorentz force F_{Lr} will be induced by the interaction of magnetic field B and the distorted current component J_r , which can be expressed as:

$$F_{Lr} = J_r \times B \quad (3)$$

Hence, a clockwise or an anticlockwise eddy of electrolyte in the surrounding area of the rod-like protrusion was induced on cathode surface(Figure 8(b,c)). The eddy became more intense with the increase of MFD, and a scouring action to the surface of rod-like structures will be generated. As a result, scouring action markedly affected the co-deposition process of particles, then constrained the growth behaviors of the rod-like structures, which even can break down original rod-like structures. The simulation results by Comsol also shows that there existed a larger eddy strength in the front of Fe-Si protrusion(Figure 9). Under the interaction of Lorenz force and magnetic field gradient force, only hummocky structures existed on the surface of coatings when the MFD increased to 1T. Fig.10 shows the formation process of hummocky protrusions in different time. When the deposition time was below 5 min, Fe-30wt%Si particles distributed on the coating surface evenly. When the depositing time reached 30 min, the Fe-Si particles were bundled together, and after the depositing time was at 60 min, the obtained surface morphology was almost same as that of at 120min(Figure 10). Therefore, the force exerted on Fe-Si particles can be deduced(Figure 11). In the initial stage, Fe-30wt%Si particles roughly

distributed on the coating surface evenly, but existing some relative larger particles or protrusions with several particles. Owing to the high magnetic susceptibility, there existed a high gradient zone of magnetic field in the vicinity of small protrusions. Therefore, Fe-Si particles in the solution will migrate to these protrusions under the effect of field gradient force. At the same time, the Fe-Si particles on the cathode surface also can be attracted to migrate to the surface of protrusions.

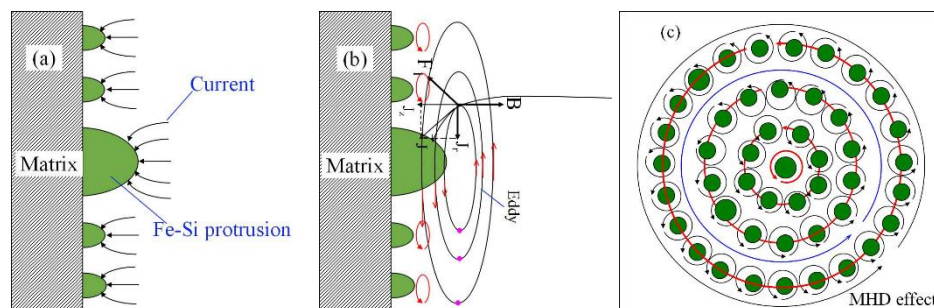


Figure 8. The schematic view of micro-MHD effect on cathode surface. (a) the distribution of electrolytic current near the rod-like structures; (b) the formation of eddies (c) eddies on the cathode surface

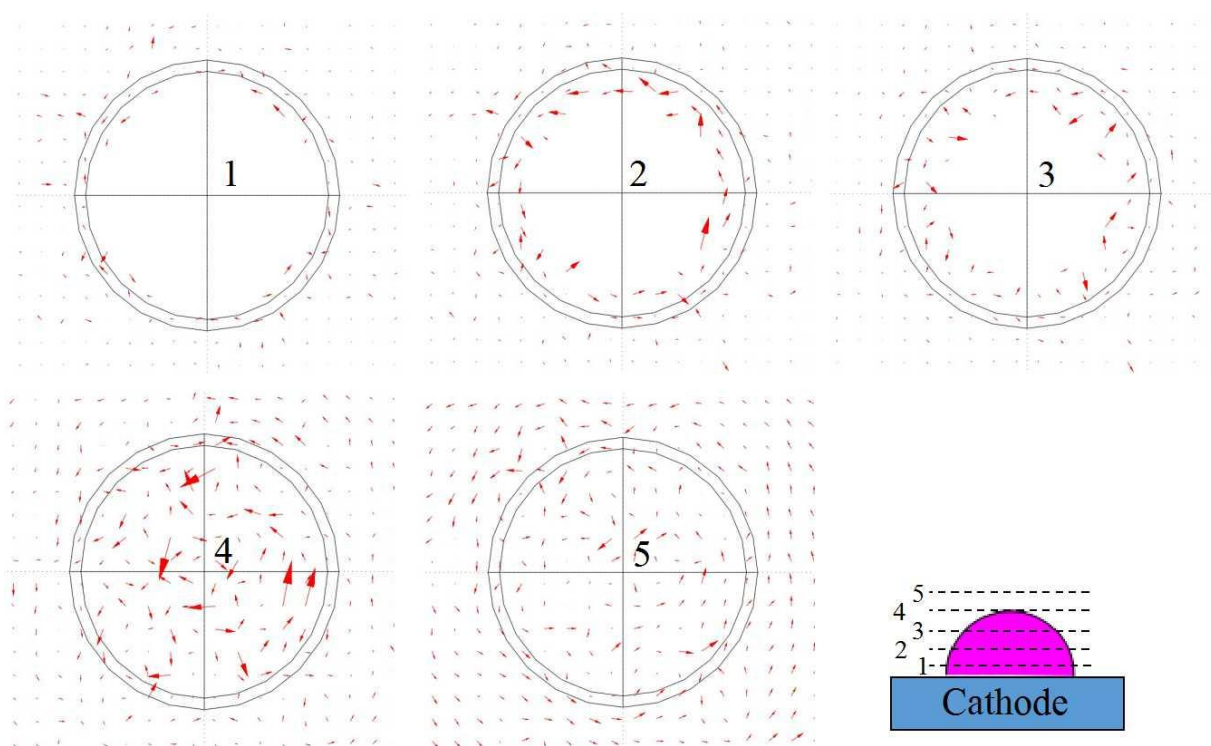


Figure 9. MHD effect was simulated by Comsol software on different depth planes of Fe-Si protrusions.

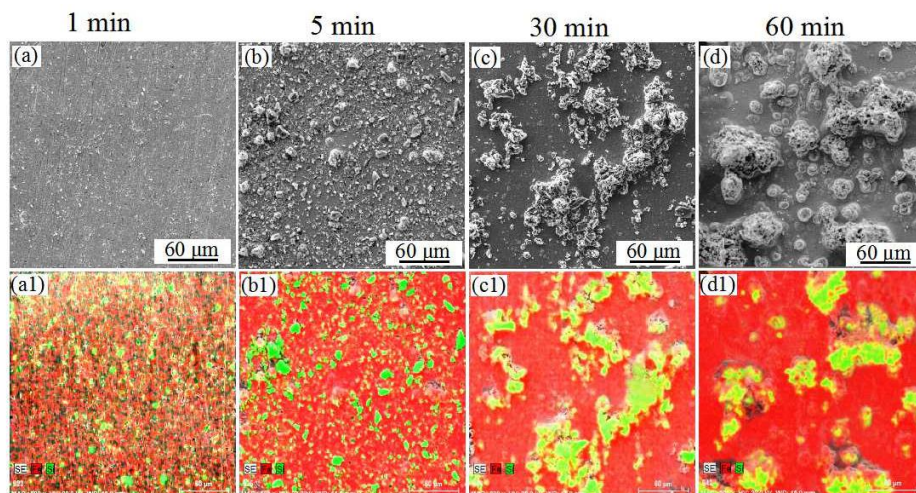


Figure 10. SEM micrographs of composite coatings and corresponding surface distribution of elements under different depositing time at $2 \text{ A} \cdot \text{dm}^{-2}$ under an 1 T magnetic field

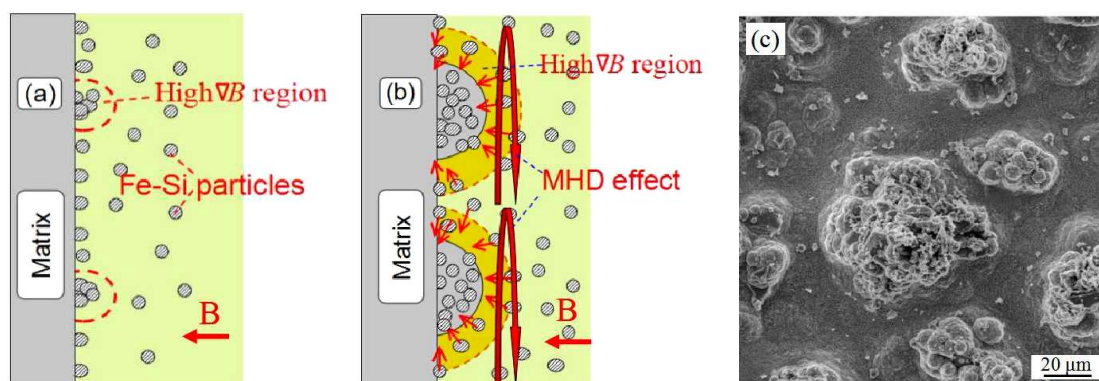


Figure 11. Formation diagram of hummocky structures for Fe-30w%Si particles in magnetic field. (a) The distribution of particles in the initial stage; (b) The interaction of field gradient force and the MHD effect; (c) Morphology of hummocky structures in 1T magnetic field

For the Si particles, the phenomenon of rod-like protrusions was not obvious. However, the MHD effect must greatly promoted the Si particles into the coatings, and some bean-like protrusions appeared on the coatings. Zhou[19] concluded that the paramagnetism of Fe^{2+} promoted that the iron atom will arrange along the direction of magnetic field and therefore induced the bean-like protrusions, that is to say the paramagnetic ions will be affected by magnetic field gradient force ($F_{0\nabla B}$). Therefore, the $F_{0\nabla B}$ to paramagnetic ions in high magnetic field should be considered and which can be expressed as[20-21]:

$$F_{0\nabla B} = \mu_0^{-1} \cdot \chi_{sol} \cdot B \cdot \nabla B \text{ with } \chi_{sol} = \sum_k \chi_{mol,k} c_k \quad (4)$$

Where χ_{sol} denotes the magnetic susceptibility of the electrolyte, χ_m denotes molar magnetic susceptibility ($\chi_{m,Fe} = 125.7 \times 10^{-9} \text{ m}^3 \text{ mol}^{-1}$). As a result, the phenomenon of bean-like structures was formed and stuck out from the coating surface. However, no bean-like structures appeared on the cathode surface during the iron deposition without any particles. After adding Si particles, with increasing current density, more bean-like protrusions appeared on the coating surface.

According to Guglielmi N[22], the particle inclusion in metallic matrix occurs in two consecutive steps of adsorption. The first step which is called "loose adsorption", ions adsorbed on the particles reversibly and yield a high degree of coverage on the electrode surface. The second step is a "strong adsorption" of the particles. The reduction of metal ions adsorbed on the particles produces the circumstance of irreversible strong adsorption. Then, these particles are engulfed by the growing metallic matrix. Above experimental results show that the particle content of coatings in a magnetic field were relatively high, which means that the loose adsorption coverage is large. Meanwhile, the conductivity of Si particles is very poor (approximately 2.52×10^{-4} S/m), which is even much lower than that of solution (approximately 4.3 S/m). Therefore, after some Si particles reached on the cathode surface, the actual current density significantly increased and led to the distribution of current in the vicinity of particles was uneven[11, 23]. As a result, some bean-like protrusions were induced on the coating surface at low current density. With increasing current density, the unevenness of current density would be aggravated, larger numbers of bean-like protrusions appeared and became increasingly evident(Figure 12). Figure 13 shows the corresponding formation process of bean-like protrusions for Si particles at different time at 2 A/dm^2 under an 1T magnetic field.

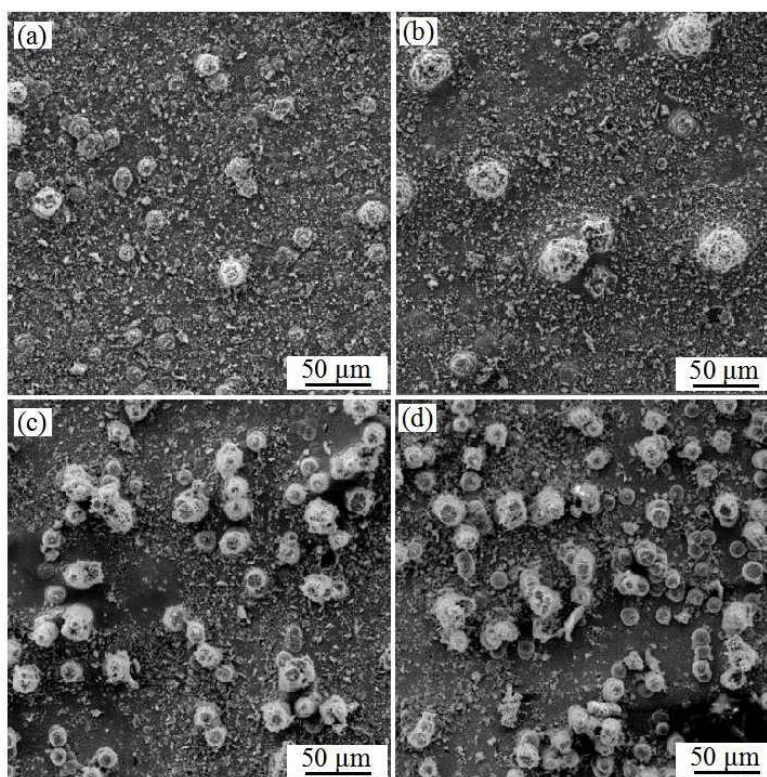


Figure 12. SEM micrographs of coating surface for Si particles under an 1 T magnetic field at different densities. (a) 0.5 A/dm^2 , 240min (b) 1 A/dm^2 , 120min (c) 3 A/dm^2 , 40min (d) 4 A/dm^2 , 30min

When the deposition time was below 5 min, Si particles distributed on the coating surface evenly in the initial stage. With increasing the depositing time, some bean-like protrusions gradually formed. When the depositing time was at 60 min, the obtained surface morphology was almost same as that of at 120min. However, no bean-like protrusions appeared on the coating surface during the iron deposition

without any particles (Figure 14). Therefore, it can be deduced that the bean-like protrusions were mainly induced by the uneven current distribution. When applying the conductive Fe-30wt%Si alloy particles, although the current distribution will be affected to a certain extent, Fe²⁺ can be reduced on cathode and particle surface after the conductive particles contacted to the cathode surface, which equivalent to increasing the discharge area of cathode surface, and therefore no bean-like protrusions appeared on the coating surface.

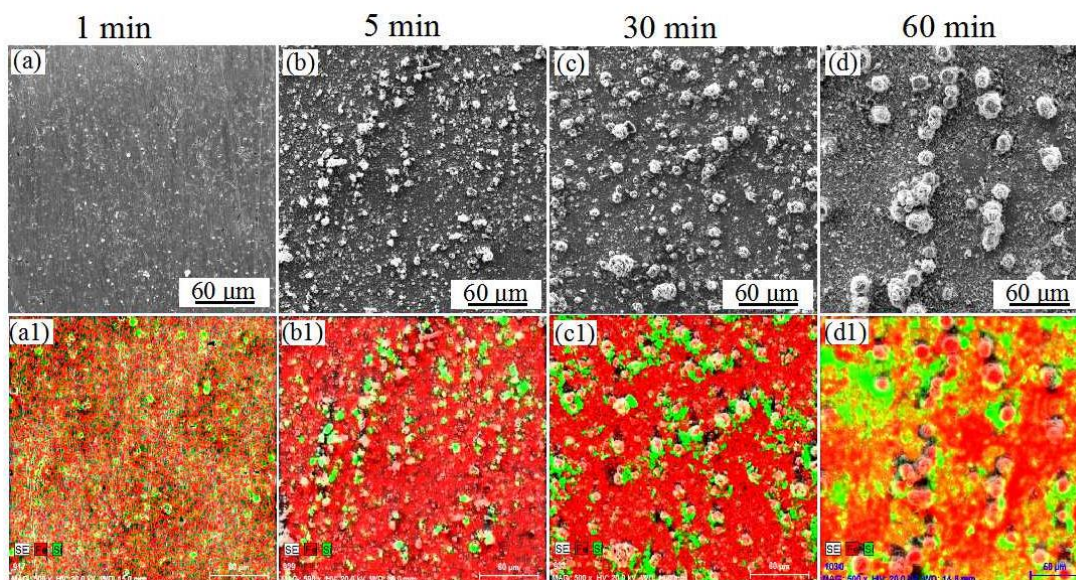


Figure 13. SEM micrographs of composite coatings and corresponding surface distribution of elements under different depositing time

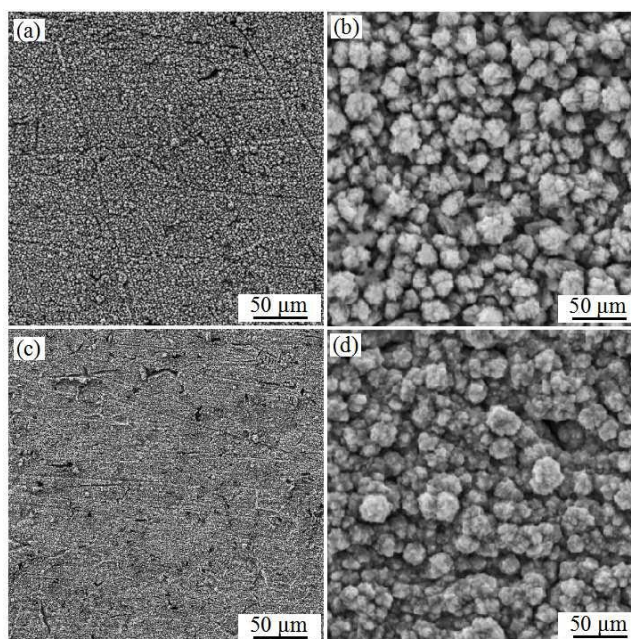


Figure 14. Surface morphology of Fe coatings in the absence of magnetic field (a-b) and in 1T magnetic field (c-d)

4. CONCLUSIONS

In this study, The Fe-Si composite coatings was prepared in magnetic field, and the co-deposition process of ferromagnetic Fe-30wt%Si and diamagnetic Si particles and their migration behavior were investigated. The main conclusions of the present study were as followed:

- Rod-like structures formed on coating surface for Fe-30wt%Si particles at relatively low MFD, and hummocky structures were gradually induced with the increase of MFD due to the synergistic effects of MHD effect and field gradient force.
- Iron bean-like structures was induced on coating surface for Si particles, largely attributed to the unevenness of local current distribution in magnetic fields.
- The silicon content of coatings for Si particles increased markedly with the increase of MFD due to the MHD effect, whereas that for Fe-30wt%Si particles maintained a basically stable state after the MFD was above 0.1T.

ACKNOWLEDGEMENTS

The authors gratefully acknowledged the financial support of national natural science foundation joint fund (U1732276; U1860202), 135 National key research and development program common technology for metallurgical process of tool and die steel(2016YFB0300401), National Natural Science Foundation of China(51664009), the Guizhou Provincial Natural Science Foundation of China(2016-7101), the Guizhou Provincial Education Department innovation group project(2016-043), and the Guizhou institute of technology project(KJZX17-015; XJGC20161212; KJZX19-002).

References

1. D. D. Ning, A. Zhang, M. Murtaza and H. Wu, *J. Alloys. Compounds*, 777 (2019) 1245.
2. Y. Liang, Z. C. Guan, H. P. Wang and R. G. Du, *Electrochem. Commun.*, 2017, 77 (2017) 120.
3. H. Krawiec, V. Vignal, A. Krystianiak, O. Heintz and M. Latkiewicz, *Surf. Coat. Technol.*, 2019, 363 (2019) 128.
4. D. Khazeni, M. Saremi and R. Soltani, *Ceram. Int.*, 45 (2019) 11174.
5. M. Y. Xu, L. D. Shen, W. Jiang, F. Zhao, Y. Chen and Z. J. Tian, *J. Alloys. Compounds*, 2019, 799 (2019) 224.
6. C. Y. Ma, X. Guo, J. Leang and F. F. Xia, *Ceram. Int.*, 42 (2016) 10428.
7. M. H. Peng, Y. B. Zhong, T. X. Zheng, L. J. Fan, J. F. Zhou, W. L. Ren and Z. M. Ren, *J Mater. Sci. Technol.*, 34 (2018) 2492.
8. P. W. Zhou, Y. B. Zhong, H. Wang, Q. Long, F. Li and Z. Q. Sun, *Appl. Surf. Sci.*, 282 (2013) 624.
9. R. Morimoto, M. Miura, A. Sugiyama, M. Miura, Y. Oshikiri, I. Mogi, S. Takagi, Y. Yamauchi and R. Aogaki, *J Electroanal. Chem.*, In press, 2019.
10. K. Nishikawa, T. Saito, H. Matsushima and M. Ueda, *Electrochim. Acta*, 297 (2019) 1104.
11. Q. Long, Y. B. Zhong, F. Li, C. M. Liu, J. F. Zhou, L. J. Fan and M. J. Li, *Acta Metall. Sin.*, 49 (2013) 1201.
12. R. Peipmann, J. Thomas, A. Bund, *Electrochim. Acta*, 52 (2007) 5808.
13. Q. Long, Y. B. Zhong, T. X. Zheng and C. M. Liu, *Chem. Res. Chinese U.*, 30 (2014) 811.
14. Q. Long, Y. B. Zhong, Y. J. Wu and Y. Z. Zhang, *Int. J. Electrochem. Sci.*, 13 (2018) 11691.
15. C. Wang, Y. B. Zhong, J. Wang, Z. Q. Wang, W. L. Ren, Z. S. Lei and Z. M. Ren, *J. Electroanal.*

- Chem.*, 630 (2009) 42.
16. C. Wang, Y.B. Zhong, W.L. Ren, Z.S. Lei, Z.M. Ren, J. Jia and A.R. Jiang, *Appl. Surf. Sci.*, 254 (2008) 5649.
 17. T. Yamada, S. Asai, *J. Jpn. Inst. Met.*, 69 (2005) 257.
 18. T. Yamada, S. Asai, *J. Jpn. Inst. Met.*, 65 (2001) 910.
 19. P.W. Zhou, Y.B. Zhong, H. Wang, L.J Fan, L.C Dong, F. Li, Q. Long and T.X. Zheng, *Electrochim. Acta*, 111 (2013) 126.
 20. K. Tschulik, R. Sueptitz, M. Uhlemann, L. Schultz and A. Gebert, *Electrochim. Acta*, 56 (2011) 5174.
 21. F. Karnbach, M. Uhlemann, A. Gebert, J. Eckert and K. Tschulik, *Electrochim. Acta*, 123(2014)477.
 22. N. Guglielmi, *J. Electrochem. Soc.*, 119(1972) 1009.
 23. Q. Long, Y.B. Zhong, F. Li, H. Wang, J.F. Zhou, W.L. Ren and Z.S. Lei, *J. Cent. South. Univ.(Chinese)*, 45 (2014) 367.

© 2019 The Authors. Published by ESG (www.electrochemsci.org). This article is an open access article distributed under the terms and conditions of the Creative Commons Attribution license (<http://creativecommons.org/licenses/by/4.0/>).